Surface polaritons on metallic wire gratings studied via power losses

Hans Lochbihler
Max-Planck-Institut für Extraterrestrische Physik, Giessenbachstraße, 85748 Garching bei München, Germany
(Received 14 November 1995)

Surface polaritons on metallic wire gratings have been investigated by studying power losses at the grating surface. The dispersion, exhibiting gaps of energy and momentum, respectively, has been obtained from calculated power losses for various grating materials and periods. The propagation mechanism of surface polaritons along this nonadjacent periodic interface and the energy gaps in the dispersion are explained by means of the Kronig-Penney model. The power losses at gold-wire gratings with different profiles have been measured by means of photoacoustic spectroscopy. The experimental results agree with the theoretical predictions. The position of the maximum surface polariton excitation yields interesting information for the characterization of the grating profile.

I. INTRODUCTION

Nonradiative surface waves which propagate along an interface between a metal and a dielectric with phase velocities less than that of light are usually labeled as surface polaritons (SP's).[1] Gratings are especially suitable for studying SP's excited by *p*-polarized light, since they can provide reciprocal lattice vectors as additional momentum for the matching of momenta in the excitation mechanism. SP's decay nonradiatively into excited single-electron states which relax under production of heat. Additionally, they can recombine into radiation by the interaction of surface roughness. Due to this ''missing'' energy, the occurrence of SP's yields singularities in the propagating diffraction orders. Conventionally, SP excitation has been studied by the observation of these singularities (or so-called resonance anomalies) in the diffracted orders. For instance, if no higher diffraction orders are present at a reflection grating, the resonant minima in the specular reflectance correspond inevitably to the enhanced power losses from SP excitation. However, if more than one order is propagating, the minima in the specular reflectance do not always coincide with the resonant maxima of power losses. The absorption of SP's can be determined quantitatively from the measured intensities of all propagating orders.[2] This procedure, however, may be quite difficult, since all diffracted orders change their position by a variation of angle or by the wavelength of the incident photons.

Alternatively, the power losses can be measured directly by means of the photoacoustic (PA) method.[3] This technique has been successfully applied by Inagaki and co-workers[4–8] to study SP excitation on silver films and sinusoidal reflection gratings. In this paper, the PA method is used for the experimental investigation of SP's on *wire gratings*.

It has been shown in a recent paper[9,10] that SP's may be excited on metallic wire gratings. This is not obvious from previous investigations of SP's on reflection gratings, since a wire grating is represented by a *nonadjacent* periodic interface. Thus, the propagation mechanism of SP's along this structure is different from that of shallow corrugated reflection gratings for which the corrugation is often considered as a small perturbation of a flat metallic surface.[11–13] In Ref. 9, the dispersion of SP's on gold-wire gratings has been investigated by locating the resonant singularities in the *transmittance* of the zeroth order. Measurements as a function of wavelength λ and angle of incidence Θ_0 have been performed by means of a spectrophotometer. $(-1,+1)$ minigaps[12] in dispersion caused by the interference of contrapropagating first order SP's have been analyzed for gratings with different wire profiles.

In this paper, the power losses on metallic wire gratings are employed for localizing SP excitations in the (λ,Θ_0) plane. Next, the dispersion is evaluated by numerical data exhibiting minigaps in the first and also in higher orders of SP modes. Furthermore, a simple model analogous to the Kronig-Penney model is developed for physical interpretation of the behavior of SP's, i.e., propagation mechanism and dispersion, on wire gratings. In the experiment section, the excitation of SP's is studied for gold gratings with different profiles by means of the PA method using a Nd:yttrium aluminum garnet (Nd:YAG) laser. For this wavelength, SP excitation is also investigated in conical (off-plane) mountings varying the polar and the azimuthal angle of incident *p*-polarized photons.

II. NUMERICAL STUDY

Figure 1 shows a sketch of a wire grating which is periodic in the *x* direction and whose wires are parallel to the *z* axis surrounded by a vacuum. The geometric parameters for this grating, which has a rectangular profile, are given by the period d, the wire width b, and the wire height h. For the optical excitation of SP's, a *p*-polarized plane wave ($\vec{E}$ vector parallel to the plane of incidence) with wave number k_0 impinges at a polar angle Θ_0 and an azimuthal angle Φ_0. SP's may be excited if the wave vector $\vec{k}_{\mathrm{SP}}$ differs from the momentum component of the incident photons $\vec{k}_0^{\parallel}$ which is parallel to the grating plane by a multiple number n of reciprocal-lattice vectors $G=2\pi/d$. For an off-plane (or conical) mounting, the *x* and *z* components of momenta have to be matched such that

$$\pm\vec{k}_{\mathrm{SP}}=k_0\begin{pmatrix}\sin\Theta_0\cos\Phi_0\\ \sin\Theta_0\sin\Phi_0\end{pmatrix}+\begin{pmatrix}nG\\ 0\end{pmatrix}. \tag{1}$$

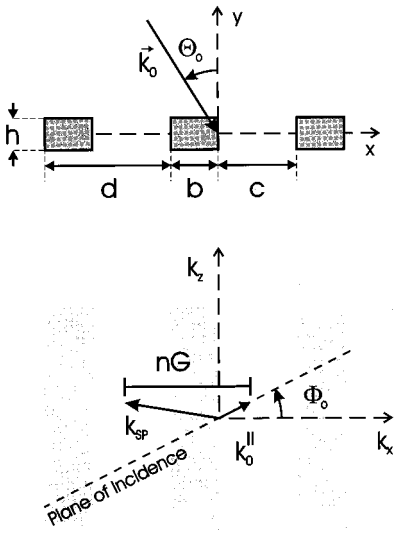

FIG. 1. The wire grating (period d, wire width b, width of free space $c=d-b$, and wire height h) is illuminated with p-polarized light at a polar angle Θ_0 and an azimuthal angle Φ_0. Surface polaritons (SP's) with wave-vector $\vec{k}_{SP}$ may be excited if the x components of $\vec{k}_{SP}$ and $\vec{k}_0$ differ by a multiple number n of reciprocal-lattice vectors $G=2\pi/d$.

For an in-plane (or classical) mounting, the z components of the wave vectors $\vec{k}_{SP}$ and $\vec{k}_0^{\parallel}$ vanish and Eq. (1) reduces to

$$\pm k_{SP}=k_0\sin\Theta_0+nG, \tag{2}$$

by matching the x components of the momenta.

The diffraction of plane waves on highly conducting wire gratings has been modeled by means of formalisms described in Ref. 14 for rectangular profiles and Ref. 15 for arbitrary cross sections. These methods utilize the surface impedance as a boundary condition on the metallic wire surface without having to calculate the electromagnetic fields inside the wires. The surface impedance boundary condition (SIBC) represents the following relation between the tangential components of the electric and magnetic fields at the boundary of a metal-vacuum interface:

$$\vec{E}_{\parallel}=Z\hat{n}\times\vec{H}_{\parallel}, \tag{3}$$

where Z is the surface impedance and $\hat{n}$ denotes a normal unit vector on the boundary pointing into the free-space side. The approximation of a constant impedance $Z=1/\sqrt{\epsilon}$ (ϵ denotes the permittivity of the metal) already yields good results for metallic wire gratings in the near infrared (NIK).[14,15] It has been shown[9] that the SIBC method appears superior to an exact formalism[16] for studying gold-wire gratings with rectangular profile in the NIR: it does not exhibit numerical difficulties, its numerical calculation time is significantly shorter, and it practically yields the same results as the exact method. Furthermore, a simple relation between the power losses and the electromagnetic fields on the metallic surface can be obtained by means of the SIBC. SP's are related to abnormally high radiation losses and they result in strong field enhancement on the grating surface.[10] The power losses normalized to the incident power P_{abs} can be derived from the second Green's identity. Imposing the SIBC, we obtain

$$P_{abs}=\frac{\mathrm{Re}Z}{d\cos\Theta_0}\oint_S|H_z|^2ds \tag{4}$$

for p-polarized light in classical mounting, whereas the integral has to be determined along the wire surface. For conical mountings ($\Phi_0\neq 0°$), it gives

$$P_{abs}=\frac{\mathrm{Re}Z}{d\cos\Theta_0}\oint_S\left[|H_z|^2+\frac{1}{(k_0^2-k_z^2)^2}\left|k_0\frac{\partial E_z}{\partial\hat{n}}-k_z\frac{\partial H_z}{\partial\hat{T}}\right|^2\right]ds, \tag{5}$$

where $\hat{T}=\hat{n}\times\hat{z}$ is the unit vector parallel to the metallic surface and $k_z=k_0\sin\Theta_0\sin\Phi_0$ is the z component of the incident wave vector.

Because of the large of number of parameters which can be varied for investigating SP's, we limited this numerical study to gratings with rectangular profiles in classical mounting. In the next section, however, gratings in conical mountings and gratings with trapezoidal profiles are also discussed. Figure 2 shows the power losses as a function of wavelength $\lambda=2\pi/k_0$ and angle of incidence Θ_0 for three different metallic wire gratings with a period $d=1$ μm and a wire rectangular wire profile ($b=0.4$ μm, $h=0.4$ μm). The grating material is in (a) gold, (b) silver, and (c) aluminum. For the numerical calculation, the optical constants of (galvanically deposited) gold have been taken from Ref. 14; those of silver and aluminum are published in Ref. 17. The positions of SP excitation have been obtained from the maxima of power losses varying the wavelength by fixed angles Θ_0. The diagrams above the plots of power losses show these dispersions of SP's in the (λ,Θ_0) plane by solid lines. The Rayleigh thresholds on which a new diffraction order is appearing (or becomes vanishing) are marked by dashed lines. This also yields to a singularity in the power losses, since the electromagnetic field is enhanced at the grating surface due to the grazing diffraction angle of the appearing (or vanishing) order. Note that these positions are equivalent to the dispersion-free propagation.

One interesting feature is the splitting at the intersections of SP dispersion branches. Two kinds of splittings have been observed for SP's on gratings: energy gaps which are caused by the interference of contrapropagating SP's resulting in standing waves and momentum gaps (k gaps) which have been attributed to finite lifetime effects and to loss of coupling strength.[12,13,18–21] Both types of gaps can be observed in Fig. 2 for the $(-1,+1)$ minigaps. The relation between the quantity of the energy gap $E_g^{(-1,+1)}$ and the wire profile has already been demonstrated in Ref. 9. Here, it is shown that $E_g^{(-1,+1)}$ depends also on the grating material, i.e., the optical constants. For the gratings discussed in Fig. 2, $E_g^{(-1,+1)}$ is 40 meV for gold, 39 meV for silver, and 33 meV for aluminum.

Momentum gaps, however, are often hard to distinguish from energy gaps.[22] This might be the reason for the continued controversy. Heitmann *et al.*,[13] Nash *et al.*,[20] and Fischer, Fischer and Knoll[19] investigated the SP excitation on sinusoidal reflection gratings. These authors, however, found

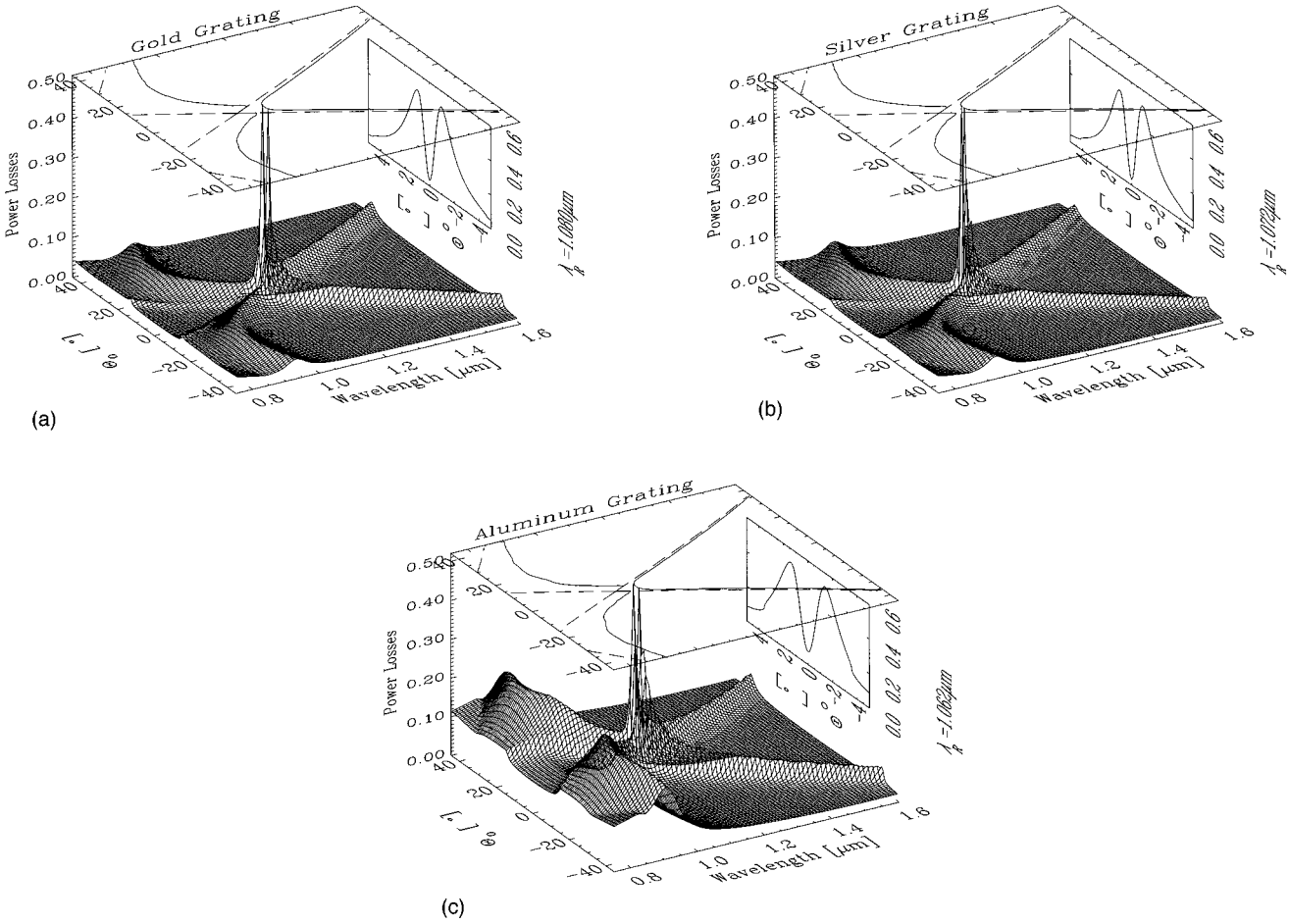

FIG. 2. Calculated power losses at wire gratings with rectangular profile ($d=1$ μm, $b=0.4$ μm, $h=0.4$ μm) as a function of wavelength and angle of incidence Θ_0 for various grating materials: (a) gold, (b) silver, and (c) aluminum. The plot above shows the disperison of SP's corresponding to the maxima of power losses (solid lines). The positions of the Rayleigh anomalies are marked by dashed lines. The plot on the right side illustrates the power losses as a function of Θ_0 for a wavelength λ_R on which the resonant maximum of power losses occurs.

different types of *k* gaps which exhibit splittings either in the higher or lower frequency branch or in both branches. As far as we know, this behavior of the dispersion curves has not yet been satisfactorily explained.

It can be seen from Fig. 2 that SP's on metallic wire gratings also exhibit *k* gaps in the crossing of $(-1,+1)$ order SP coupling branches. The lower frequency branch has a maximum of SP coupling near normal incidence at which the power losses are about 50%. The plots on the right-hand side of the three-dimensional (3D) diagrams represent intersections through these resonance maxima at wavelength λ_R as a function of angle Θ_0. The position of this maximum depends on the grating material. For gold, the maximum occurs at 1.0°, for silver at 0.9°, and for aluminum at 1.4°. In normal incidence, however, the coupling to SP's vanishes totally. Clearly, no momentum transfer parallel to the grating plane is possible. On the other hand, the higher frequency branch does not exhibit this sharp resonance feature. The coupling to SP's is obviously weaker. However, the power losses become much lower as soon as *both* first diffraction orders become evanescent. Therefore, the solid lines of the dispersion end at the dashed lines, representing the Rayleigh thresholds. From this behavior, one can conclude that photons couple to SP's by a kind of umklapp process, i.e., by a momentum transfer of reciprocal-lattice vectors from a diffraction order which propagates in the opposite *x* direction as the SP's.

In Fig. 3, the numerically calulated power losses of a gold-wire grating with a period $d=2$ μm are shown in the near infrared. The cross section is a rectangle with a width $b=0.653$ μm and a height $h=0.556$ μm. Due to the larger period, the $(\pm 1,\mp 2)$ minigaps and parts of the $(-2,+2)$ and $(\pm 1,\mp 3)$ minigaps can be observed. An energy gap of 30 meV has been found in the crossing of $(-1,+1)$ order SP branches; $E_g^{(\pm 1,\mp 2)}$ is 97 meV in the $(\pm 1,\mp 2)$ minigaps. Generally, the coupling strength decreases for higher coupling modes. Compared with the gold grating from Fig. 2, the SP resonance at wavelength $\lambda_R=2.115$ μm is sharper due to the higher conductivity. Furthermore, the *k* gap is apparently smaller. In the crossing of $(-2,+2)$ order SP branches, however, no *k* gap occurs in spite of the normal incidence of the photons. The coupling by the umklapp process to SP's, i.e., coupling of the first propagating diffraction orders via reciprocal-lattice vectors, explains this phenomenon.

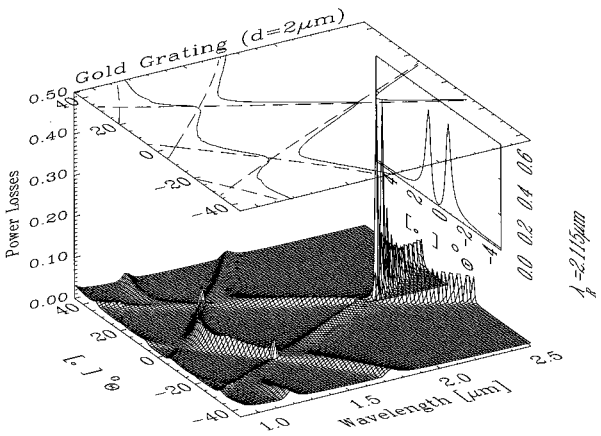

FIG. 3. Same as Fig. 2 for a gold-wire grating with a period $d=2$ μm and rectangular profile ($b=0.663$ μm and $h=0.556$ μm).

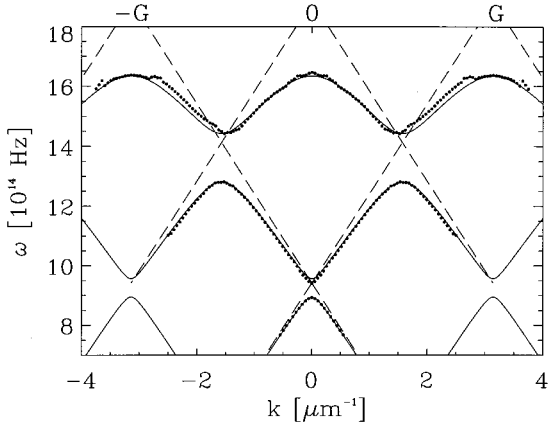

FIG. 4. Dispersion of SP's on grating from Fig. 3 in an extended Brillouin-zone scheme: KP model (solid lines) and data are evaluated from the numerical calculated maxima of power losses (dots). The Rayleigh thresholds are marked by dashed lines.

The results presented above are based on the numerical solution of Maxwell's equations plus boundary conditions at wire gratings. Unfortunately, it is not possible to derive simple formulas from those formalisms in order to join to a detailed physical insight for the behavior of SP's. Hence, a simplified model is now presented which explains the dispersion and the energy gaps of SP's on wire gratings.

A simple model for dispersion of SP's

It is well known that the behavior of particles in a periodic square-well potential can be described by the Kronig-Penney (KP) model.[23] For this one-dimensional model, the wave equation can be solved in terms of simple analytic functions. SP's traveling along a wire grating are influenced by a periodic potential. We assume that the SP's propagate along the grating seeing a periodic piecewise constant potential which is different for the regions of the metallic wires and for the free-space regions between the wires.

The (complex) wave number q of the electromagnetic waves within the region of the metallic wires can be approximated by

$$\epsilon\chi_0+\chi\frac{1\mp\exp i\chi h}{1\pm\exp i\chi h}=0, \tag{6}$$

with

$$\chi_0^2=k_0^2-q^2 \text{ and } \chi^2=\epsilon k_0^2-q^2. \tag{7}$$

This relation corresponds to the dispersion of SP's on a metallic film[1] with thickness h. The sign for the roots χ_0 and χ is chosen so that $\mathrm{Re}\chi_0+\mathrm{Im}\chi_0>0$ and $\mathrm{Re}\chi+\mathrm{Im}\chi>0$. The SP's on the upper and the lower surface are no longer coupled if $\mathrm{Im}\chi\gg 1/h$. Thus, Eq. (6) simplifies for highly conducting films with thicknesses larger than a fraction of one vacuum wavelength to

$$q=k_0\sqrt{\frac{\epsilon}{\epsilon+1}}, \tag{8}$$

which is equivalent to the dispersion of SP's on a flat metallic surface.

The free-space regions between the wires represent inhibited zones for the SP's. Thus, they cross these regions by a tunneling process having a wave number κ for which $|\mathrm{Im}\kappa|>|\mathrm{Im}q|$. Then, by imposing the boundary conditions at the interfaces $x=0,c$ and by employing Floquet's theorem, the dispersion can be evaluated analytically[23] giving

$$-\frac{1}{2}\left(\frac{q}{\kappa}+\frac{\kappa}{q}\right)\sin(qb)\sin(\kappa c)+\cos(qb)\cos(\kappa c)=\cos(k_{\mathrm{SP}}d), \tag{9}$$

where k_{SP} is the wave vector of the SP's. After developing the trigonometric functions on the left-hand side of Eq. (9), the energy gaps at $\cos(k_{\mathrm{SP}}d)=\pm 1$ can be easily estimated from the roots of a quadratic equation.

This simplified model for the dispersion of SP's on wire gratings, however, suffers the drawback that the wave number κ cannot be derived by simple terms. Nevertheless, this value can be found by fitting Eq. (9) to measured dispersions or numerically calculated dispersions obtained from Maxwell's equations. A comparison of both dispersions is illustrated in Fig. 4 for a gold-wire grating with the same parameters as used in Fig. 3. In this extended Brillouin-zone scheme, the dispersion evaluated from the maxima of power losses (see solid lines in the upper plot of Fig. 3) is marked by dots. Again, the dispersion-free propagation coincident with the Rayleigh thresholds is shown by dashed lines. From Eq. (9), the dispersion of SP's has been obtained using $\kappa=k_0+10\mathrm{Re}(q-k_0)+i220\mathrm{Im}q$ (solid lines). It must be noted that this value for κ is not generally valid for gratings with rather different wire profiles and grating materials, since, in this one-dimensional model, the parameter wire height is not involved. In addition, the propagation of SP's in the free-space regions between the wires is actually more complicated, as can be seen from the energy flow diagrams in Ref. 10. This is also the reason for the remaining discrepancies between both dispersion obtained from numerically calculated power losses and the results of Eq. (9). However, the proportionality of E_g to the normalized width of the free-space region c/d shown in Ref. 14, and also the fact that E_g increases for higher coupling orders, can be explained by means of this model.

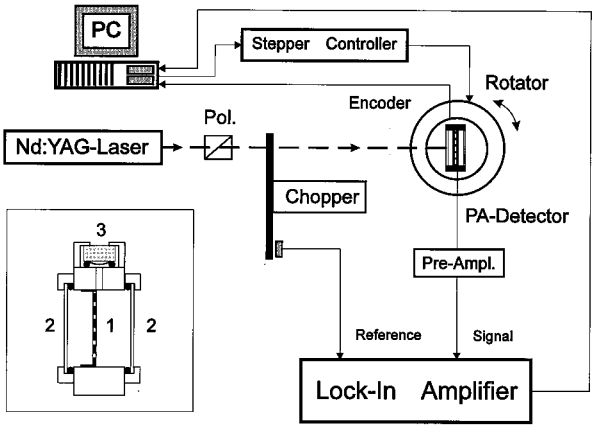

FIG. 5. Sketch of the experimental setup for the PA measurements. A cross-sectional view of the PA cell is illustrated in the inset. 1: grating, 2: glass windows, and 3: microphone.

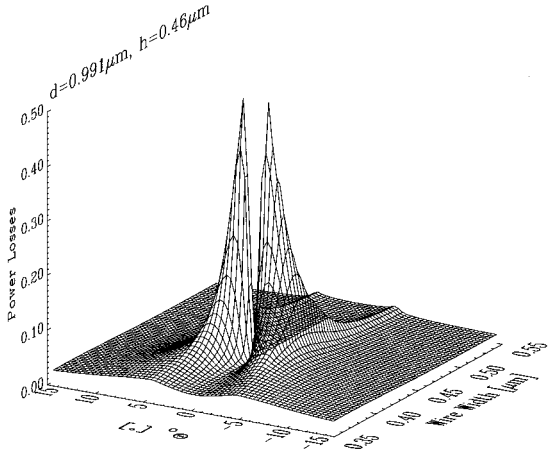

FIG. 6. Calculated power losses at a gold-wire grating with rectangular profile ($d=0.991$ μm, $h=0.46$ μm) as a function of angle of incidence Θ_0 and wire width b for a wavelength $\lambda=1.064$ μm. The azimuthal angle is $\Phi_0=0°$.

Finally, it should be noted that the lower frequency branches in the vicinity of the $(\pm 3,\mp 1)$ minigaps and the $(-2,+2)$ minigap degenerate in a similar manner as experimentally shown by Chen *et al.*[12] for sinusoidal silver gratings.

III. EXPERIMENT

The wire gratings have been manufactured from gold by means of a photochemical process.[24] The gratings discussed in this section have a period of $d=0.991$ μm and their wire profile is approximately rectangular. For better mechanical stability, this wire structure is overlayed by a rough support grid and fixed in a metallic frame.

The photoacoustic method has been utilized for studying the absorption of p-polarized light on these gratings. The experimental setup for the PA measurements is sketched in Fig. 5. The grating is mounted in an air-filled PA cell with a total gas volume of 2.4 cm^3 (see inset of Fig. 5). The cavity is sealed air tightly with rubbers and is in contact with an electret microphone (Sennheiser KE 13-227), whose sensitivity is 35.5 mV/Pa. Photoacoustic signals can be generated if the sample is illuminated by a chopped laser beam through the highly transparent glass window. The transmitted radiation leaves the PA cell through the exit window. For this study, the p-polarized beam of a diode-pumped Nd:YAG laser ($\lambda=1.064$ μm) with 20-mW power was directed onto the PA cell. PA measurements as a function of angle of incidence were performed by tilting the PA detector with a stepper rotator. A personal computer controls the stepper motor and reads out the data coincidently from the lock-in amplifier and the angle encoder.

The relation between heat generation due to light absorption and the production of the photoacoustic signal can be described by a one-dimensional model developed by Rosencwaig and Gersho.[3] In the present experiment, the thermal diffusion length of gold is much larger than the thickness of the gratings. Therefore, the PA signal is expected to be proportional to absorbed power and has a f^{-1} dependence on the chopper frequency f. Furthermore, it has to be pointed out that the absorbed power is very effectively converted into PA signals for these grating samples since they are free standing and have no backing material.

The linearity of the PA detector has been experimentally confirmed by varying the incident laser power for one grating at different angles of incidence. For the PA measurements, the chopper frequency was set to $f=80$ Hz. Finally, the measured data have been corrected for the power losses at the glass windows and the support structure of the grating.

Results

The power losses have been measured by means of the above-described setup for a large number of gold-wire gratings with different wire profiles. For brevity, we only present data for gratings with an approximately rectangular profile and constant wire height. Figure 6 shows the numerical results of the power losses at gold-wire gratings with rectangular profiles and a height $h=0.46$ μm as a function of angle of incidence Θ_0 and wire height h for in-plane mounting ($\Phi_0=0°$). At wavelength $\lambda=1.064$ μm, the power losses on a gold surface are typically a few percent. Similar to Figs. 2 and 3, a sharp absorption peak appears near normal incidence due to SP excitation. The maximum of power losses of about 50% occurs for a wire width $b=0.426$ μm at angle $\Theta_0=1.26°$.

The PA signals, as a function of angle of incidence Θ_0, have been measured at four gratings whose profiles distinctly differ in wire width. The geometry parameters of the wire profile have been reconstructed by fitting an electromagnetic model to transmittance measurements.[15] It has been assumed that the geometry of the profile is trapezoidal, characterized by the medium width b, height h, and slope of the sides s (for a rectangle $s=90°$). The wire width is $b=0.435$ μm for grating 1055, $b=0.448$ μm for grating 1089, $b=0.509$ μm for grating 898, and $b=0.549$ μm for grating 918. For all of these gratings the wire height is $h=0.46\pm 0.01$ μm and the slope is $s\geq 85°$. Figure 7 shows a comparison between the measured PA signals and calculated power losses for these gratings, whereas the scalings have been chosen such that the numerical results can be directly compared with the experimental data. The SP resonance becomes obviously weaker for gratings, with increasing wire width. This confirms the

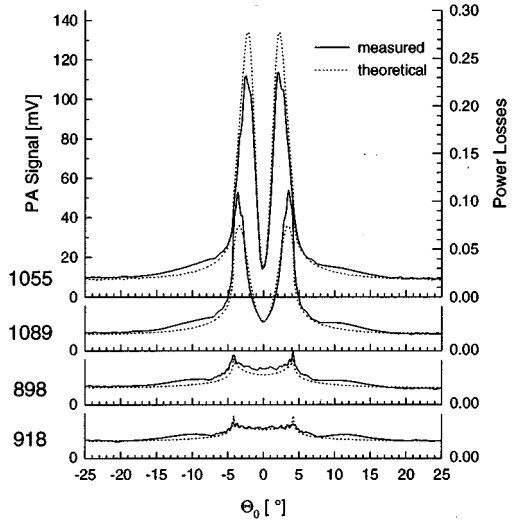

FIG. 7. Comparison between measured photoacoustic signals and calculated power losses for four different gold-wire gratings with a period $d=0.991$ μm. Grating 1055: $b=0.435$ μm, $h=0.468$ μm, $s=85°$. Grating 1089: $b=0.448$ μm, $h=0.455$ μm, $s=87°$. Grating 898: $b=0.509$ μm, $h=0.453$ μm, $s=86°$. Grating 918: $b=0.549$ μm, $h=0.452$ μm, $s=86°$.

relationship between the wire width and the position and strength of the SP resonance shown in Fig. 6. However, there are two kinds of discrepancies between theory and measurements. First, at angle $\Theta_0 \approx \pm 10°$, the PA signal is slightly higher than predicted by the numerical calculations for all gratings since a part of the first propagating diffraction orders is absorbed at the walls of the PA cell and, therefore, contributes to the PA signal. Second, the measured power losses in the maximum of SP resonance differ distinctly from the numerical results for gratings 1055 and 1089. Inagaki, Kagami, and Arakawa[4] observed a disprepancy between the absorbance $(1-R-T)$ and the nonradiative decay of SP's on silver films. They attributed the missing part of absorbance to the *radiative* decay of SP's due to interaction with surface roughness. However, in this experiment, no significant scattering arising from surface roughness was observed. Moreover, for grating 1089 too much power loss in the maximum of SP resonance has been measured, as predicted by the numerical calculations. Furthermore, the coincidence of the theoretical with the measured peak position indicates that the wire profile is correctly fitted. Attempts to fit more complicated geometries of wire profiles did not remove this discrepancy. The origin of this discrepancy might be due to lateral fluctuations of the wire width. Considering the numerical data in Fig. 6, a full width at half maximum (FWHM) of 10 nm has been found for the power losses as a function of wire width at angle $\Theta_0=1.26°$. Clearly, if this narrow peak is broadened by a variation of wire width, the power losses become lower in the maximum and rise in the sides. Even a fluctuation in a scale of nanometers can explain that discrepancy between measurement and the numerical results.

In a similar manner, the influence of the wire height on the SP resonance maximum has been investigated. The position and the strength of the SP resonance also depends on the wire height, but it is less sensitive to variations of wire

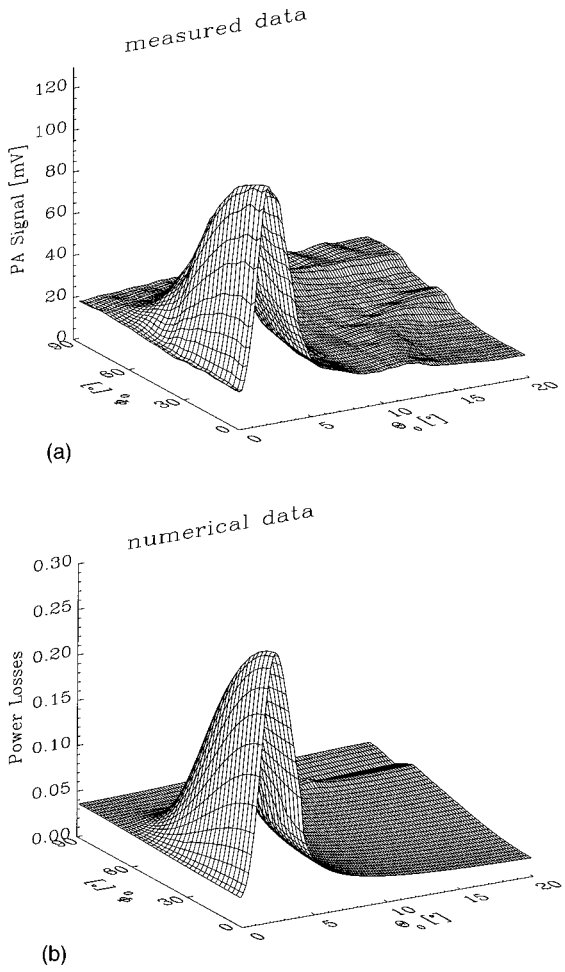

FIG. 8. Power losses at the grating 1055 ($d=0.991$ μm) as a function of polar angle Θ_0 and azimuthal angle Φ_0 for the wavelength $\lambda=1.064$ μm. (a) Measured photoacoustic signal and (b) numerical calculation assuming a rectangular wire profile with parameters $b=0.434$ μm and $h=0.462$ μm.

height compared with variations of wire width. For instance, the FWHM of the SP resonance for a gold grating with a wire width $b=0.43$ μm is 40 nm at $\Theta_0=1.35°$.

Finally, the power losses have been studied for gold-wire gratings in *conical* mountings. In this experiment, the PA signal has been measured as a function of polar angle Θ_0 and azimuthal angle Φ_0 of incident p-polarized photons at wavelength $\lambda=1.064$ μm. Measured data, as well as numerical results, are shown in Fig. 8 for the grating 1055. In the numerical calculations, it has been assumed that the wire profile is a rectangle with a width $b=0.434$ μm and height $h=0.462$ μm. The resonant maximum of power losses nearly obeys a $\cos^2\Phi_0$ law, since only the field component whose $\vec{E}$ vector vibrates perpendicular to the surface of the grating wires can couple to SP's. For increasing azimuthal angles Φ_0, the peak position is shifted towards larger polar angles Θ_0 in the measurement, as well as in the calculated data. This shift of the SP resonance angle can also be determined from Eq. (1), since the x component of the photon momentum is constantly varying Φ_0 for a certain SP mode.

IV. CONCLUSIONS

The power losses, rather than the efficiency of the zeroth order, have been employed to study photon-induced SP's on metallic wire gratings. The power losses as a function of wavelength and angle of incidence have been calculated for gratings made of different metals with periods of 1 μm and 2 μm, respectively. The dispersion of SP's has been determined from the maxima of power losses. The dispersions exhibit splittings at the crossings of contrapropagating SP modes. These minigaps have been examined in detail for the first and also for the higher SP coupling modes. The SP's on metallic wire gratings behave similarly to particles in a periodic square-well potential which can be described by the KP model. From this one-dimensional model, the dispersion-exhibiting energy gaps in the center and the edge of the reduced Brillouin zone have been derived by simple analytic terms. This model explains the proportionality of the quantity of the energy gap E_g to the normalized width of the free-space region c/d and to the number of coupling order. The origin of the observed k gaps is attributed to the absence of momentum transfer from photons to SP's. SP's might also be excited via the umklapp process from photons in the propagating diffraction orders. This explains the k gap in the higher frequency branch of the $(-1,+1)$ minigap and the absence of a k gap in the $(-2,+2)$ minigap.

The power losses on gold-wire gratings with a period of ≈ 1 μm and different wire profiles have been measured by PA spectroscopy at $\lambda = 1.064$ μm. The measurements agree well with the numerical calculations. Remaining discrepancies are due to lateral fluctuations of the wire profile. It has been found that the SP resonance peak can be sensitive for the geometry parameters of the profile within nanometer scalings. Thus, the measurement of this SP resonance peak can provide interesting information about the wire profile. Furthermore, the power losses have also been investigated for conical mountings through experimentation, as well as through numerical calculations. For increasing azimuthal angles of incidence Φ_0, the coupling to SP's becomes weaker and vanishes if the $\vec{E}$ vector of the incident photons vibrates parallel to the grating wires. The shift of the SP peak towards larger angles Θ_0 for increasing Φ_0 results directly from the momentum equation.

[1] *Surface Polaritons*, edited by V. M. Agranovich and D. L. Mills (North-Holland, Amsterdam, 1982); H. Räther, *Surface Plasmons on Smooth and Rough Surfaces and on Gratings* (Springer-Verlag, Berlin, 1988).

[2] M. C. Hutley and V. M. Bird, Opt. Acta **20**, 771 (1973).

[3] A. Rosencwaig, *Photoacoustics and Photoacoustic Spectroscopy* (Wiley, New York, 1980).

[4] T. Inagaki, K. Kagami, and E. T. Arakawa, Phys. Rev. B **24**, 3644 (1981); Appl. Opt. **21**, 949 (1982).

[5] T. Inagaki, M. Motosuga, K. Yamamori, and E. T. Arakawa, Phys. Rev. B **28**, 1740 (1983).

[6] T. Inagaki, M. Motosuga, E. T. Arakawa, and J. P. Goudonnet, Phys. Rev. B **31**, 2548 (1985).

[7] T. Inagaki, J. P. Goudonnet, J. W. Little, and E. T. Arakawa, J. Opt. Soc. Am. B **2**, 433 (1985).

[8] T. Inagaki, J. P. Goudonnet, and E. T. Arakawa, J. Opt. Soc. Am. B **3**, 992 (1986).

[9] H. Lochbihler, Phys. Rev. B **50**, 4795 (1994).

[10] H. Lochbihler, Opt. Commun. **111**, 417 (1994).

[11] R. H. Ritchie, E. T. Arakawa, J. J. Cowan, and R. N. Hamm, Phys. Rev. Lett. **21**, 1530 (1968).

[12] Y. J. Chen, E. S. Koteles, R. J. Seymour, G. J. Sonek, and J. M. Ballantyne, Solid State Commun. **46**, 95 (1983).

[13] D. Heitmann, N. Kroo, C. Schulz, and Zs. Szentirmay, Phys. Rev. B **35**, 2660 (1987).

[14] H. Lochbihler and R. A. Depine, Appl. Opt. **32**, 3459 (1993).

[15] H. Lochbihler and R. A. Depine, Opt. Commun. **100**, 231 (1993); J. Mod. Opt. **40**, 1273 (1993).

[16] L. C. Botten, M. S. Craig, R. C. McPhedran, J. L. Adams, and J. R. Andrewartha, Opt. Acta **28**, 1087 (1981); **28**, 1103 (1981).

[17] J. H. Weaver, C. Krafka, D. W. Lynch, and E. E. Koch, *Optical Properties of Metals* (Fachinformationszentrum Energie, Physik, Mathematik GmbH, Karlsruhe, 1981), Pt. 2, No. 18-2.

[18] V. Celli, P. Tran, A. A. Maradudin, and D. L. Mills, Phys. Rev. B **37**, 9089 (1988); P. Tran, V. Celli, and A. A. Maradudin, Opt. Lett. **13**, 530 (1988).

[19] B. Fischer, T. M. Fischer, and W. Knoll, Appl. Opt. **34**, 5773 (1995).

[20] D. J. Nash, N. P. K. Cotter, E. L. Wood, G. W. Bradberry, and J. R. Sambles, J. Mod. Opt. **42**, 243 (1995).

[21] W. L. Barnes, T. W. Preist, S. C. Kitson, J. R. Sambles, N. P. K. Cotter, and D. J. Nash, Phys. Rev. B **51**, 11 164 (1995).

[22] M. G. Weber and D. L. Mills, Phys. Rev. B **34**, 2893 (1986).

[23] R. de L. Kronig and W. G. Penney, Proc. R. Soc. London **110**, 499 (1931); C. Kittel, *Solid State Physics* (North-Holland, Amsterdam, 1982), Vol. 6.

[24] H. Bräuninger, H. Kraus, H. Dangschat, P. Predehl, and J. Trümper, Appl. Opt. **18**, 3502 (1979).